Brief Communication: Inferring Glacier Equilibrium Line Altitudes in ~~Central~~ the European Alps with FROST

Oskar Herrmann[1], Veena Prasad[1], Anna Zöller[1], Alexander R. Groos[1], Samuel Cook[1], Christian Sommer[1], and Johannes J. Fürst[1]

[1]Institute of Geography, Friedrich-Alexander-Universität Erlangen-Nürnberg, Germany

Correspondence: Oskar Herrmann (oskar.herrmann@fau.de)

Abstract. ~~Glaciers in Central Europe are projected to almost disappear by 2100. To improve projections, glacier models must be calibrated to match observations~~The current pace of glacier retreat in the European Alps is unprecedented in the observational record and has significant implications for water resources and downstream ecosystems. Quantifying the future evolution of these systems requires physically based glacier models that are calibrated against observational data. Using the open-source `Framework for assimilating Remote-sensing Observations for Surface mass balance Tuning (FROST)`, we infer ~~equilibrium-line altitudes (ELAs) and surface mass balance~~ mean Equilibrium Line Altitudes (ELAs) and other Surface Mass Balance (SMB) parameters for 409 Alpine glaciers ~~during 2000–2019 through~~ for the timer period 2000–2019 using an Ensemble Kalman Filter. The method combines an elevation-dependent ~~surface mass balance~~ SMB model with ice dynamics from the Instructed Glacier Model (IGM). Validation against ELA estimates from in-situ ~~mass balance~~ measurements and end-of-summer snowline data ~~(correlations of 0.76 and 0.62) shows that~~ shows good agreement, with Pearson correlation coefficients of $r = 0.74$ and $r = 0.64$, respectively. These results demonstrate that `FROST` enables satellite-based ~~regional estimates of glacier equilibrium conditions~~calibration of SMB parameters at regional scale and pave the way for the calibration of more complex SMB models. The framework is inherently suited for transient data assimilation, with the ultimate aim of improving the digital representation of glacier systems.

1 Introduction

Mountain glaciers are losing mass worldwide in response to anthropogenic climate change (The GlaMBIE Team, 2025) and are currently among the largest contributors to sea-level rise, comparable to the combined meltwater from Greenland and Antarctica (Slater et al., 2021). In the European Alps, roughly 4,000 glaciers were cataloged around the year 2000 (RGI Consortium, 2023), but most are projected to disappear by the end of the century due to climate change (Zekollari et al., 2025) or have already disappeared. At present, ~~these glaciers are vital for~~ glaciers in the European Alps play important roles in local hydrology (Koboltschnig and Schöner, 2011) ~~, hydroelectric power (Schaefli et al., 2019), and hazard management (Haeberli et al., 2017)~~ and hydroelectric power generation (Schaefli et al., 2019). In Switzerland alone, around 200,000 people live in areas directly influenced by glacier meltwater, glacial lakes, or periglacial processes (Huss et al., 2017). Their retreat has already shifted seasonal runoff patterns (Huss and Hock, 2018), increased ~~slope instability (Deline et al., 2015; Islam et al., 2025)~~the risk of

landslides (Haeberli et al., 2017), and led to the formation of new proglacial lakes. Underscoring , underscoring the urgency to better understand their evolution and associated risks in this densely populated region.

Accurate modeling of glacier evolution requires a realistic representation of both the surface mass balance Surface Mass Balance (SMB) and the ice dynamics. The SMB quantifies all processes of surface accumulation and melt. Existing SMB models range from simple temperature-index approaches to physically based energy balance models (?). Since the publication of Hugonnet et al. (2021)(Hock et al., 2019). At the scale of individual glaciers or catchments, a wider range of calibration data is typically available, including in-situ observations and weather stations. In contrast, at regional to global scales, SMB model calibration has often aimed to match a is more weakly constrained and has often relied on matching scalar geodetic mass balance (Maussion et al., 2019; ?)estimates derived from datasets such as Hugonnet et al. (2021), for example in Open Global Glacier Model (OGGM) v1.6 (Maussion et al., 2023), PyGEM (Rounce et al., 2023), or more recently on snowline altitude (Cremona et al., 2025). However, theses approaches strongly reduces these approaches strongly reduce the spatial information contained in modern remote-sensing products, such as elevation change or velocity fields (Hugonnet et al., 2021; Sommer et al., 2020). Efficient methods are therefore needed to assimilate such spatially distributed datasets directly into the calibration process.

The representation of ice dynamics is equally essential for glacier modeling. Flow-line models remain widely used due to their computational efficiency and ability to reduce glacier geometry to its key dimensions: length, thickness, and surface elevation along a central flow line (Maussion et al., 2019; ?). With the (Maussion et al., 2019; Rounce et al., 2023). In an recently published study of Schmitt et al. (2025) they add inversion of thickness along the flowline to OGGM based surface elevation, volume estimate and elevation change. This approach moves towards data assimilation, where multiple observational constraints are combined to infer consistent glacier states. The recent development of the IGM (?)(Jouvet and Cordonnier, 2023) , it has become feasible to simulate three-dimensional glacier flow at reasonable computational cost. IGM also enables the inversion for ice thickness and basal sliding , which are essential for constraining the internal glacier structure and basal conditionsan additional sliding coefficient field that represents unresolved processes influencing surface velocity that are not explained by ice thickness or bed slope alone. While satellite-based velocity products are increasingly available (Friedl et al., 2021; Millan et al., 2022), they are rarely used for model calibration in large-scale glacier modeling frameworks.

Ensemble-based data assimilation methods such as the Ensemble Kalman Filter (EnKF) (Evensen, 1994) have gained traction in glaciology for parameter and state estimation. The EnKF offers a derivative-free alternative to adjoint-based methods (Higdon et al., 2012; Iglesias et al., 2013)(Higdon et al., 2012; Iglesias et al., 2013; Schmitt et al., 2025), which, in contrast, require gradient computations and full access to the model internals. Applications include ensemble transform Kalman filter-based parameter estimation (Bonan et al., 2014) and assimilation of surface observations in ice sheet models (Gillet-Chaulet, 2020). Variational approaches, such as adjoint methods (Goldberg and Heimbach, 2013), remain powerful but computationally demanding. Recent work by Knudsen et al. (2024) and Herrmann et al. (2025) demonstrated the potential of EnKF for calibrating SMB parameters in a synthetic glacier setting.

Building on the `FROST` introduced by Herrmann et al. (2025), we apply it to calibrate SMB model parameters against elevation-change observations from 2000–2019 2000–2019 for the 409 glaciers in Central Europe which the European Alps

that exceeded 1 km^2 in ~~2000.~~ RGI7. This size threshold is chosen to ensure that glacier areas are sufficiently large to resolve spatial patterns in elevation change and SMB relative to observational noise. The framework combines the three-dimensional glacier evolution model IGM with an EnKF to iteratively calibrate elevation-dependent SMB parameters~~and quantify their uncertainties~~. This approach enables the calibration of glacier-specific ELAs and mass-balance gradients, where the ELA represents the ~~climatic boundary between~~ altitude separating accumulation and ablation and the gradients describe how these processes vary with elevation. We focus on ~~long-term~~ 20-year spatial patterns of accumulation and ablation, ~~as multi-year~~ because elevation-change observations over a longer time period provide more robust constraints compared to shorter periods (e.g., 5-year). The inferred ELAs are validated against independent End-of-Summer Snow Line Altitude (EoS SLA) derived from remote sensing (Sommer et al., 2026) and in-situ SMB measurements from GLAMOS (2023) and WGMS (2024), demonstrating that ~~provides consistent, observation-constrained estimates of glacier equilibrium conditions across the European Alps~~FROST enables satellite-based calibration of SMB parameters at regional scale. This study provides a simplified test case for transient data assimilation, where observations are assimilated at their time of acquisition. This enables a more accurate simulation of glacier systems and leverages the growing availability of remote sensing data. The framework is readily extendable in this direction, as the underlying EnKF is inherently designed for sequential data assimilation. By reducing the complexity of the problem to one observation period, we provide a first step toward identifying challenges on the way to fully transient data assimilation in glacier modeling.

2 Data and Method

The ~~FROST calibration~~ FROST v1.0.0 pipeline (Herrmann et al., 2025) integrates the IGM ~~(?)~~v3.0.0 (Jouvet and Cordonnier, 2023)) with the EnKF (Evensen, 1994) to estimate glacier-specific SMB parameters. The SMB model used here is an elevation-dependent piecewise-linear function and does not take climate variables as input (Eq. 1).

$$SMB(z) = \begin{cases} \beta_{acc} \cdot (z - z_{ELA}) & \text{if } z > z_{ELA}, \\ \beta_{abl} \cdot (z - z_{ELA}) & \text{otherwise.} \end{cases} \tag{1}$$

where z denotes the elevation of the glacier surface, z_{ELA} the ELA, β_{acc} and β_{abl} the accumulation and ~~the ablation gradient~~ ablation gradients, respectively. The EnKF is used to iteratively update SMB parameters by minimizing the misfit between modeled and observed elevation change. The prior distributions of the SMB parameters are derived from the GLAMOS dataset, with mean values over eleven glaciers during 2000–2019: $z_{\mathrm{ELA}} = 3144 \pm 166\,\mathrm{m}$, $\beta_{\mathrm{abl}} = 7.55 \pm 2.68\,\mathrm{m\,a^{-1}\,km^{-1}}$, and $\beta_{\mathrm{acc}} = 3.09 \pm 1.13\,\mathrm{m\,a^{-1}\,km^{-1}}$. The initial ensemble spread for every glacier is set to three times these standard deviations. It is worth noting that IGM assumes a constant ice density of 910 kg m^{-3}. A detailed description of the ~~FROST~~FROST ~~methodology~~ is provided in Herrmann et al. (2025).

The framework utilizes OGGM-shop to download, align, and pre-process surface elevation (Crippen et al., 2016), surface velocity (Millan et al., 2022), thickness measurements (Welty et al., 2020), and glacier outlines from the ~~RGI Consortium (2023)~~

RGI7 (RGI Consortium, 2023). The IGM ~~inversion for thickness and sliding coefficient includes~~ v3.0.0 inversion for ice thickness and basal sliding includes several optimization parameters, which ~~is~~ were manually tuned based on ~~the~~ examples provided in the IGM repository~~, aiming~~ . The goal was to balance the tendency to overestimate thickness for small glaciers against underestimation for large glaciers. ~~We use~~ A first qualitative assessment was based on visual inspection (e.g. Figure S4). Since the inversion of 409 glaciers is computationally costly, we tested a small number of different parameter sets and selected the one that provided the best agreement with observed surface velocities. This evaluation was based on summary statistics, including the mean, quantiles, and extremes of the velocity distributions.

As a calibration target for the EnKF, we use the elevation-change ~~observations~~ product from Hugonnet et al. (2021), which ~~provide globally gridded glacier-wide~~ provides globally gridded elevation change rates between 2000 and ~~2019.~~ 2019 at 100 m resolution. These rates are added to the NASADEM ~~2000~~ elevation data to reconstruct the 2019 surface topography, with the associated uncertainties in elevation change propagated into the 2019 elevation uncertainty. The ~~method can be easily extended to other regions because we chose this global dataset~~chosen calibration parameters, whose roles are described in more detail in Herrmann et al. (2025), are an ensemble size of 36, an elevation bin size of 50 m, and six iterations. The exact code is available at https://github.com/FAU-glacier-systems/FROST/tree/main/experiments/central_europe_submit.

For validation, we compare the calibrated SMB parameters with ~~glaciological measurements provided by~~ independent glaciological measurements from GLAMOS (2023) and WGMS (2024). Multi-year mean ELA values and SMB gradients are derived from ~~the~~ elevation-binned mass balance ~~product. As these measurements are not used in the calibration process, they serve as an independent reference for assessing the physical plausibility of our inferred parameters. We select~~ data by computing the 20-year mean for each elevation bin and fitting a bilinear function separated at the ELA. We added an explanatory figure to the supplement (Fig. S10). For the a meaningful accumulation gradient, we require a minimum of three elevation bands with positive mass balance. To ensure representative estimates of the period, we only include glaciers with more than ~~five~~ ten years of ELA ~~data to ensure a stable, representative value for~~ observations. Based on our sampling analysis, this corresponds to an average uncertainty of approximately 25 m relative to the 20-year ~~period~~mean, with occasional outliers reaching up to 100 m (see Fig. S5).

To further evaluate the inferred ELAs, we compare them to ~~. The snow lines of glaciers in the European Alps are estimated using optical remote sensing images from the~~ End-of-Summer Snow Line Altitude (EoS SLA) derived from Landsat and Sentinel-2 ~~satellite missions. We distinguish~~ imagery (Sommer et al., 2026). The distinction between areas of bare glacier ice and snow cover ~~by automatically estimating~~ is automatically estimated by intensity thresholds from infrared reflectance histograms based on Otsu's method ~~Otsu (1979)~~(Otsu, 1979). Thereby, the glacier area covered by snow is identified due to the relatively high near- (NIR) and shortwave-infrared (SWIR) reflectance of snow compared to bare ice or debris ~~Hall et al. (1987)~~ (Hall et al., 1987). The date-specific snow line altitude is then derived by masking the surface elevations of the NASADEM with the pixels ~~of each satellite image that are~~ classified as snow. For each glacier and year, the EoS SLA is defined as the highest transient snowline observed during the late ablation season (15 ~~August~~July–30 September). Estimates based on fewer than three suitable satellite scenes were subjected to outlier detection, as a minimum of three scenes is required to ensure sufficient temporal coverage of the late ablation period. For glaciers with at least ten valid years, values deviating by more than

±3 ±2 standard deviations from the glacier-specific mean were removed. For ; for glaciers with fewer than ten valid years, an additional physical threshold was applied, excluding excluded EoS SLAs differing by more than 400 m from the mean glacier elevation (RGI v7). The mean EoS SLA for 2000–2019 2000–2019 was then computed from all non-flagged years . As serves as a proxy for annual , the dataset provides and serves as an independent benchmark for evaluating the calibrated ELA values.

We restrict the comparison to glaciers larger than 1 km^2, and assess agreement For more details we refer to Sommer et al. (2026) . The comparison is assessed using the Pearson correlation coefficient (Eq. **??**) and mean absolute error.

$$r = \frac{\sum_{i=1}^{n}(x_i - \bar{x})(y_i - \bar{y})}{\sqrt{\sum_{i=1}^{n}(x_i - \bar{x})^2}\sqrt{\sum_{i=1}^{n}(y_i - \bar{y})^2}}$$

where y_i are the observed values, x_i the corresponding calibrated or modeled values, $\bar{x}$ and $\bar{y}$ their respective means, and n the number of paired samplesMean Absolute Error (MAE).

3 Results

We applied the workflow method described in Section 2 to the glaciers in Central Europe the European Alps and calibrated glacier specific ELA for this region409 glaciers. Here, we summarize regional patterns, validation against the GLAMOS dataset dataset from Glacier Monitoring Switzerland (GLAMOS) and World Glacier Monitoring System (WGMS), and compare with EoS SLA extracted from optical imagery.

3.1 Regional equilibrium line altitude distribution

Our calibration results yield an ELA range of from 2540 to 3540 m a.s.l. for the Alps in the period 2000-2019period 2000–2019, with a mean of 3158 m a.s.l. and a standard deviation of 157 m. The spatial distribution of modeled ELAs reflects the main climatic gradients across the Alps: lower values occur along the northern and western flanks, while higher values dominate in the higher inner Alps (Fig. 1). The equivalent maps for the calibrated gradients are provided in the supplements (Fig. S2 and S3). While ELAs correlates correlate with mean glacier elevation, no other systematic relation relationship with glacier size or aspect emerges at the scale of the entire Alps (see Supplementary MaterialFig. S1), although in some subregions the observed spread is likely influenced by hypsometry and exposure. Local deviations can further arise from shading, debris cover, and other surface or topographic effects, which were not investigated in this study.

3.2 Validation with end-of-summer snow line altitude

The close match between modeled and observed elevation change demonstrates that the filter effectively combines observations and model output mean elevation change of the individual glaciers show a strong agreement (Fig. 2a). Figure 2b shows that , with a correlation of $r = 0.88$ and a MAE of $0.13\,\mathrm{m\,yr^{-1}}$. Also the ELA correlation with EoS SLA-based proxies exhibit a similar spatial pattern, as indicated by a Pearson correlation of 0.62. The mean absolute error of 217 m is largely 0.64. The

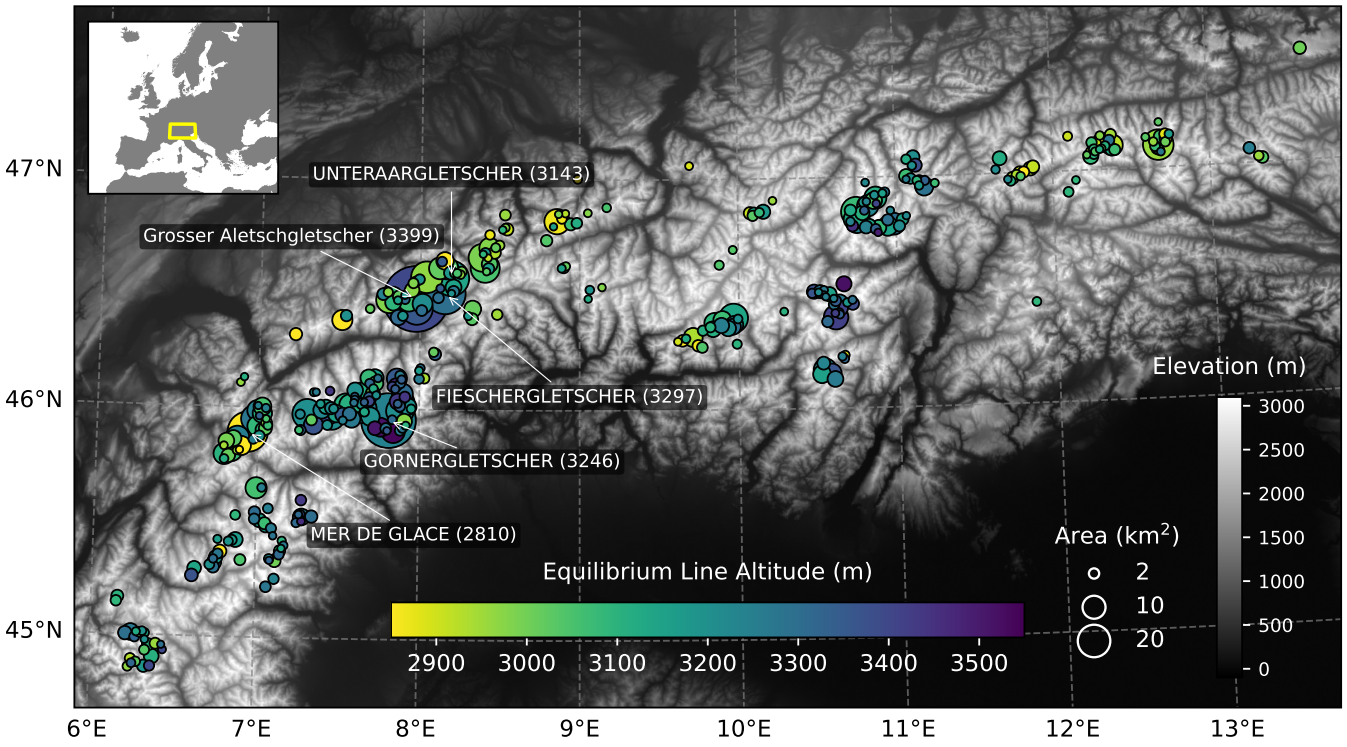

Figure 1. ~~Coloured circles show the mean~~ Mean ELA of glaciers in the European Alps for the period ~~2000–2019~~2000–2019, calibrated using ~~FROST~~FROST. ~~The background topography~~ Circle color indicates the ELA, and circle size is ~~taken from~~ proportional to glacier area. Five large glaciers are labeled with their names and the calibrated ELA in parentheses. Background topography © EuroGeographics.

MAE of 180 m is partly driven by a bias of ~~190 m. This bias~~ +135 m, which can be attributed to a systematic underestimation of the EoS SLA, since the underlying imagery ~~typically does not~~ do not necessarily capture the day of maximum snowline retreat. After ~~applying a bias correction(subtracting the bias from each calibrated ELA so that both sets have the same mean) the mean absolute error decreases to 129 m~~ bias correction, the MAE decreases to 126 m (MAE*) (Fig. 2b).

3.3 Validation against glaciological observations

The modeled and observed ELAs ~~cluster around the diagonal, indicating a~~ show consistent agreement across a range of ~~different glaciers(Fig. 3a). Only the Grosser Aletschgletscherhas a much higher calibrated~~ glaciers, with $r = 0.74$ and a MAE of 97 m. The only notable outlier is Grosser Aletschgletscher, where the calibrated ELA (3399 m a.s.l.) ~~than observed~~ substantially exceeds the observed value (3034 m a.s.l.)~~. Modeled and observed gradients show however, less correlation (Fig. 3b,c). Reasons are diverse and include variations in ablation gradients driven by local ice-flow dynamics, as well as poorly constrained accumulation gradients, since many glaciers in this region have only small or no-longer-extant accumulation areas.Consequently,~~. The mass balance gradients show considerably weaker agreement: the ablation gradient yields $r = 0.12$

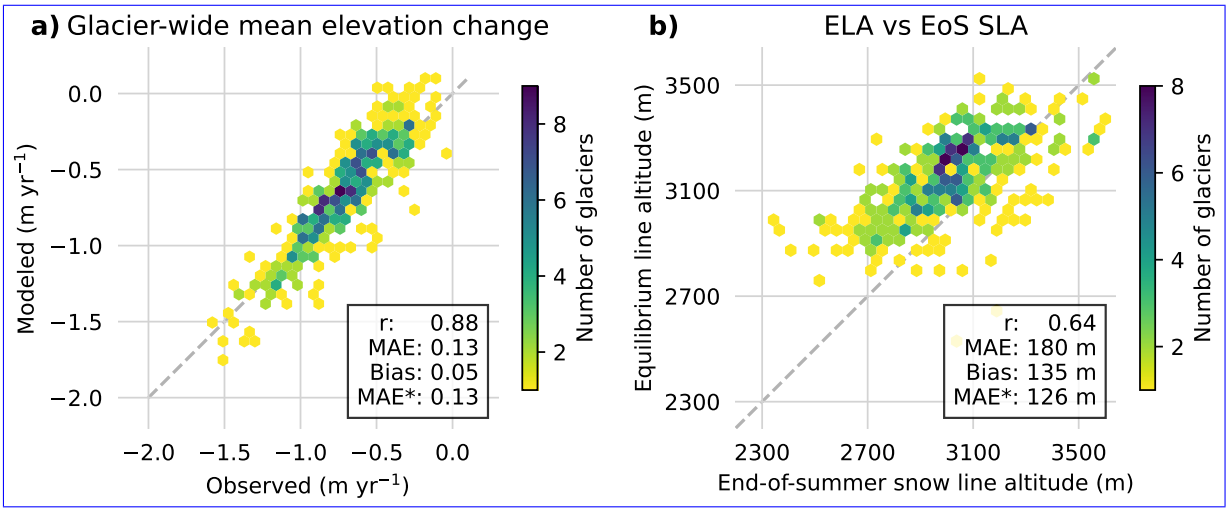

Figure 2. Comparison with observed glacier-wide elevation change (Hugonnet et al., 2021) and End-of-Summer Snow Line Altitude (EoS SLA). Panel a shows modeled and observed elevation change, and panel b shows ~~modeled~~ calibrated ELA and EoS SLA. Both panels use hexagon density plots, where color indicates the number of glaciers per bin. The total sample number is 409. Pearson correlation coefficients (r), MAE, and ~~mean absolute errors~~ bias-corrected MAE (MAE*) are ~~given~~ reported in each panel.

and a MAE of 4.07 m w.e. yr^{-1} km^{-1}, and the accumulation gradient ~~has little influence on the overall elevation change . Reasons for the deviation of the ablation gradients are discussed in Section 4.~~

~~The correlation between the~~ $r = 0.22$ and a MAE of 1.56 m w.e. yr^{-1} km^{-1}. Modeled and observed mean elevation change are in good agreement ($r = 0.94$, MAE = 0.12 m w.e. yr^{-1}), as expected since it is used as the calibration target. The Hugonnet et al. (2021) elevation change dataset ~~(used for calibration) and~~ and the glaciological mass balance observations ~~(used for evaluation)supports the comparison of calibrated parameters against parameters derived from (Fig. 3e). We acknowledge that volume change and mass change are not identical, but their strong correlation allows deviations to help explain mismatches in the calibrated parameters. The agreement of the~~ show a strong correlation ($r = 0.74$), supporting the use of the former as a calibration target and the latter as an independent evaluation dataset. The ice-dynamic parameters ~~underlying the calibration suggests that~~ show broad agreement with observations that are used in the ice-dynamic ~~constraints are broadly consistent (~~calibration, with $r = 0.77$ for ice thickness and $r = 0.61$ for surface velocity. Grosser Aletschgletscher is an outlier in both thickness and velocity, and Plaine Morte is an additional outlier in the thickness comparison. These results are summarized in Fig. 3~~f-h). However, this agreement reflects similarity in meanvalues, while spatial distributions can differ substantially. It should also be noted that thickness measurements are sparse, and the modeled thickness can deviate from reasonable values in areas without observations~~. The velocity comparison between modeled and observed values for all glaciers, along with additional metrics including mean, quantiles, and extremes, is shown in Fig. S4.

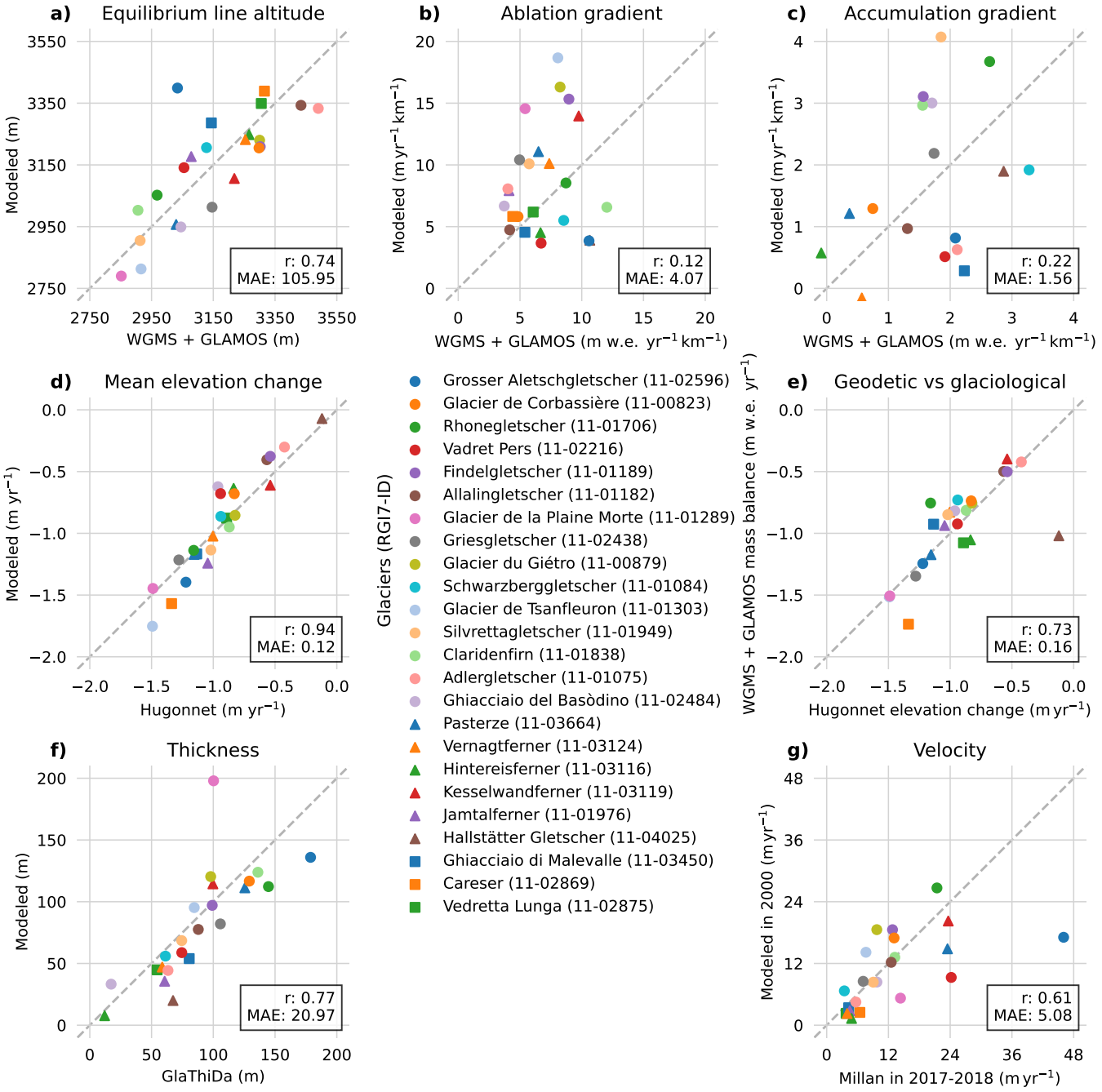

Figure 3. Validation against glaciological observations. Sub-panels show (a) ~~ELA~~ELA, (b) ablation gradient, (c) accumulation gradient, (d) mean elevation change used as ~~EnKF~~ EnKF target, (e) comparison of calibration target and evaluation data, (~~e~~ hf) ~~ice-dynamic parameters~~ ice thickness, and ~~product consistency~~(g) surface velocity. Pearson correlation coefficients and ~~mean absolute errors~~ MAE are ~~given~~ reported in each panel. Circles indicate glaciers in Switzerland, triangles in Austria, and squares in Italy.

4 Discussion

The results demonstrates that the FROST enables regional, observation-constrained calibration of SMB parameters and ELAs across the European Alps. At the same time, the results highlight several limitations related to inversion settings, input data quality, and model assumptions. In the following, we discuss the main sources of inaccuracies and their impact on the calibrated parameters, and place the simplified experimental design of this study in the context of future developments toward fully transient data assimilation.

UNIFORM INVERSION SETTINGS Achieving consistency between observed and modeled glacier velocity and thickness typically requires glacier-specific tuning of the IGM inversion parameters. Applying a single parameter set to all 409 glaciers inevitably stretches the inversion~~'~~'s capabilities, as no systematic procedure for automated tuning currently exists and manual adjustment for each glacier is not feasible. After extensive testing, we adopted a compromise parameter set for IGM ~~3.0~~v3.0.0~~(available at)~~, balancing the tendency to overestimate thickness in small glaciers against underestimation in large ones. ~~The~~ A visual indicator for the regional agreement with velocity observation were Fig. S4. Grosser Aletschgletscher is particularly affected~~, as~~ : at 81 km^2 it is by far the largest glacier in the ~~sample with an area of 81 km^2 (~~dataset, with the second largest, ~~Glacier de Corbassière, covers 16~~Pasterze, covering 18.5 km^2~~). For such large glaciers, the current inversion performs less accurately, and an adapted~~ . The current inversion settings result in an underestimated ice thickness and surface velocity for Aletschgletscher (Fig. S5), and the consequently reduced ice flux is compensated by a lower ablation gradient in the calibration. An adapted inversion parameter set would yield more realistic ice-dynamic parameters and, in turn, more physically consistent SMB calibration. However, to maintain a broadly applicable workflow, we ~~use~~ retain a uniform parameter set. ~~A more adaptive method would certainly improve the ice-flow parameters~~ Future versions of IGM are expected to be less sensitive to parameter settings and, in ~~turn, the calibration of the parameters~~general, more robust in reproducing the observed velocity field and inferring realistic thickness fields.

~~Inaccuracies in the input datasets~~ INACCURACIES IN THE INPUT DATASETS Observation errors can propagate through the calibration. Elevation-change products such as Hugonnet et al. (2021) rely on temporal aggregation and may exhibit ~~regional biases~~local biases, particularly in accumulation areas with low surface contrast and steep slopes, where small horizontal errors can translate into large vertical offsets. We also observed unrealistically high velocity patches in the surface velocity fields from ~~Millan et al. (2022)~~ Millan et al. (2022) for several glaciers~~(Plaine Morte , Glacier de Tsanfleuron,)~~, including Plaine Morte (Fig. S6) and Glacier du ~~Gietro). Such artifactscan introduce inconsistencies between modeled and actual ice dynamics and may partly explain the stronger calibrated ablation gradients, as excessive ice transport toward the glacier front requires~~ Giétro (Fig. S7). These processing artifacts, in combination with uniform inversion settings, lead to unrealistically high ice fluxes towards the glacier tongue. This increased flux is compensated by higher ablation rates~~to match the observed elevation changes~~, which drives the calibrated ablation gradient to unrealistically large values. This mechanism likely contributes to the weak agreement in the ablation gradient ($r = 0.12$, MAE $= 4.07$ m w.e. yr^{-1} km^{-1}) reported above, with Plaine Morte and Glacier du Giétro representing extreme cases.

~~The simplification of the~~ ASSUMPTIONS OF THE SMB MODEL The elevation-dependent SMB ~~models to the elevation~~

only neglects the model neglects horizontal variability. This reduction to elevation is a common assumption in regional and global-scale glacier modeling. Although SMB and elevation change are primarily governed by elevation, lateral differences are not represented and can be significant, particularly in branching glaciers where flow and mass balance vary across within the same elevation band due to azimuth, shading and small-scale precipitation variability. The piecewise linear parameterization of the mass balance profile is a reasonable first-order approximation, but does not fully capture the nonlinear altitudinal variability observed in glaciological measurements (see Fig. S10). These simplifications may contribute to the weak agreement in the ablation gradient. The accumulation gradient is additionally poorly constrained, as most glaciers in the European Alps have lost much of their accumulation area over the period 2000–2019, leaving few observations to anchor the gradient. However, since the accumulation gradient has a relatively minor influence on the overall mass balance compared to the ablation gradient and ELA, this limitation is of secondary concern.

SIMPLIFIED TEMPORAL REPRESENTATION The current study does not implement a fully transient data assimilation framework, but instead relies on a simplified setup using a single observation period (2000-2019). This implies that temporal inconsistencies between input datasets are not explicitly accounted for. In particular, the velocity product and RGI outlines may represent different periods, and potential glacier slowdown in the 21st century is not captured. Similarly, ice thickness observations are assumed to represent the glacier state in 2000, although they originate from years around 2000. These limitations may affect the consistency of inferred parameters and initial conditions. Extending the framework toward a fully transient data assimilation scheme that integrates time resolved observations represents an important direction for future work.

EVALUATION DATASETS Validation against EoS SLA-based proxies and GLAMOS glaciological mass balance observations may show deviations that do not necessarily indicate calibration errors, but rather reflect that these products represent related, yet not identical, quantities. EoS SLA data are spatially aggregated and sensitive to threshold definitions, while GLAMOS mass balance data from GLAMOS and WGMS rely on interpolation between sparse stake measurements and may not capture localized variability. Despite these limitations, the regional agreement demonstrates that the workflow captures the main climatic and topographic controls on For glaciers with limited temporal coverage (e.g., only 10 ELA across the Alps.

Overall, the analysis highlights that the FROST framework reproduces key climatic and geometric dependencies of glacier mass balance, yet remains sensitive to initialization and data quality. Future developments should first address the initialization through improved inversion strategies and, once a stable initialization is achieved, focus on integrating transient dataassimilation methods to assimilate observations at their acquisition timeobservations within the study period, such as Glacier de la Plaine Morte and Glacier de Tsanfleuron), the sampling uncertainty can reach up to 100 m. A finer temporal resolution of the SMB model would allow direct comparison with point measurements. In contrast, our evaluation is based on aggregated and processed glaciological data.

5 Conclusion

~~We present a regional workflow to calibrate~~ The presented framework provides a regional calibration of SMB parameters ~~representing~~ for the period 2000–2019, including estimates of ELAs for all glaciers larger than 1 km^2 ~~across~~ in the European Alps~~in the year 2000. The approach integrates glacier modeling within an framework and is evaluated against independent observations from and derived from optical satellite imagery.~~

~~The workflow successfully reproduces~~ . Overall, the analysis demonstrates that the FROST reproduces SMB parameters and large-scale ELA patterns across the Alps, ~~showing~~ with good agreement with ~~glaciological observations~~ independent observations from GLAMOS and WGMS, and consistent relationships ~~to~~ with EoS SLA. ~~This demonstrates that the approach captures the main climatic and topographic controls on glacier mass balance at a regional scale. Deviations in ablation and accumulation gradients reveal remaining~~ At the same time, the results highlight limitations. The ~~simplified elevation-based~~ framework remains sensitive to data quality and the initialization of ice dynamics, with inaccuracies in the input datasets and thickness inversion propagating into the calibrated parameters. Future versions of IGM are expected to reduce these effects and improve SMB ~~model and uniform inversion parameters currently limit FROST's performance. Inaccuracies in input data affect the calibration. Global velocity products can locally overestimate motion on small glaciers, introducing inconsistencies and partly explaining stronger calibrated ablation gradients.~~ parameter estimates.

~~Overall, the~~ The Python-based, ~~fully~~ open-source ~~FROST framework demonstrates~~ framework integrates IGM within an EnKF and offers strong potential for ~~calibrating glacier models with remotely sensed observations. Future developments should aim to improve the IGM inversion through glacier-specific or adaptive parameter tuning and to better account for initialization-related ice-dynamic effects. The framework is open to other data sources of elevation change or ice velocity. Combining multiple data-sources is a great potential of the framework reducing uncertainties of observations~~combining multiple remote sensing datasets. Here, we restrict the assimilation to a single observation period, providing a simplified test case. However, the EnKF naturally enables sequential assimilation and the incorporation of observations at their time of acquisition. Extending the framework toward transient data assimilation, including repeated elevation-change observations, snowline data, or surface velocities, is a logical next step. With these ~~refinements,~~ advances, ~~FROST~~FROST ~~will enable more robust assimilation of time-dependent observations for regional glacier~~ can enable more consistent and robust, observation-driven calibration of glacier models for regional monitoring and projection.

Code availability. The workflow presented in this study is implemented in the open-source FROST framework, available under a permissive license at https://github.com/FAU-glacier-systems/FROST. The underlying ice-flow inversion uses IGM version 3.0.0 (Jouvet and Cordonnier, 2023), which is also publicly available at https://github.com/jouvetg/igm. All scripts required to reproduce the regional calibration experiments and figures are archived with the publication (see Supplement).

Data availability. The Hugonnet et al. (2021) elevation-change dataset is publicly available from https://doi.org/10.6096/13. Glacier outlines are taken from RGI v7.0 (RGI Consortium, 2023), accessible at https://www.glims.org/RGI/. Surface Velocity data is available from Millan

et al. (2022) and thickness measurements form Welty et al. (2020). Glacier-specific reference mass-balance data are provided by GLAMOS (GLAMOS, 2023) and the WGMS (WGMS, 2024). The datasets are available at https://doi.org/10.18750/massbalance.2020.r2021 and https://doi.org/10.5904/wgms-fog-2026-02-10. The EoS SLA data set is available at https://doi.org/10.5281/zenodo.18223929 and the repository containing the processing scripts at https://github.com/cr-sommer/snowy-glaciers.

Author contributions. OH designed the study, performed the model runs, and analyzed the results. VP, AZ, and SC contributed through discussions that improved the understanding and application of the glacier model and provided input on the workflow. CS and ARG provided the EoS SLA data, including a description of its derivation from remote sensing observations. CS contributed expertise on remote sensing and ARG provided expertise on the interpretation of glaciological measurements and surface mass balance properties. JJF assisted with model implementation, supervised the project, and contributed to the conceptual framing. All authors discussed the results and contributed to the writing of the manuscript.

Competing interests. Johannes J. Fürst is a member of the editorial board of TC.

Acknowledgements. OH, VP, ARG, and JJF received primary funding from the European Union's Horizon 2020 research and innovation programme via the European Research Council (ERC) as a Starting Grant (FRAGILE project) under grant agreement No. 948290. AZ acknowledges support from the Response project (DFG Individual Research Grant No. 495516510). SC acknowledges funding from the Elitenetzwerk Bayern through the DeLIGHT project. The processing of data on snow-line elevation based on remote-sensing images was financially supported by the Dr. Hertha & Helmut Schmauser Research Foundation as part of the funded proposal *"Automated measurement of seasonal snow cover on glaciers using time-series analysis of optical satellite data in Google Earth Engine."*

This research was supported by the M^{3}OCCA graduate school and by computational resources provided by the NHR@FAU. We thank the developers of OGGM and IGM for providing the modeling tools on which this work builds. We also thank GLAMOS and WGMS for providing reference mass-balance data and the RGI consortium for making glacier outlines openly available. We acknowledge Hugonnet et al. (2021) and Millan et al. (2022) for making elevation-change and ice-velocity data accessible and are especially grateful to Romain Hugonnet for guidance on the interpretation of observed elevation-change uncertainties.

Parts of the manuscript were refined using ChatGPT (OpenAI~~, version October 2025) to improve clarity and wording~~) for language editing. All scientific content and interpretations were developed ~~and verified~~ by the authors.

References

Bonan, B., Nodet, M., Ritz, C., and Peyaud, V.: An ETKF approach for initial state and parameter estimation in ice sheet modelling, Nonlinear Processes in Geophysics, 21, 569–582, https://doi.org/10.5194/npg-21-569-2014, 2014.

Cremona, A., Huss, M., Landmann, J. M., Marty, M., van der Meer, M., Ginzler, C., and Farinotti, D.: Seasonal mass balance drivers for Swiss glaciers over 2010–2024 inferred from remote-sensing observations and modelling, EGUsphere, pp. 1–27, https://doi.org/10.5194/egusphere-2025-2929, 2025.

Crippen, R., Buckley, S., Agram, P., Belz, E., Gurrola, E., Hensley, S., Kobrick, M., Lavalle, M., Martin, J., Neumann, M., Nguyen, Q., Rosen, P., Shimada, J., Simard, M., and Tung, W.: NASADEM GLOBAL ELEVATION MODEL: METHODS AND PROGRESS, The International Archives of the Photogrammetry, Remote Sensing and Spatial Information Sciences, XLI-B4, 125–128, https://doi.org/10.5194/isprs-archives-XLI-B4-125-2016, 2016.

Deline, P., Gruber, S., Delaloye, R., Fischer, L., Geertsema, M., Giardino, M., Hasler, A., Kirkbride, M., Krautblatter, M., Magnin, F., McColl, S., Ravanel, L., and Schoeneich, P.: Chapter 15 - Ice Loss and Slope Stability in High-Mountain Regions, in: Snow and Ice-Related Hazards, Risks, and Disasters, edited by Shroder, J. F., Haeberli, W., and Whiteman, C., Hazards and Disasters Series, pp. 521–561, Academic Press, Boston, ISBN 978-0-12-394849-6, https://doi.org/10.1016/B978-0-12-394849-6.00015-9, 2015.

Evensen, G.: Sequential data assimilation with a nonlinear quasi-geostrophic model using Monte Carlo methods to forecast error statistics, Journal of Geophysical Research: Oceans, 99, 10 143–10 162, https://doi.org/10.1029/94JC00572, 1994.

Friedl, P., Seehaus, T., and Braun, M.: Global time series and temporal mosaics of glacier surface velocities derived from Sentinel-1 data, Earth System Science Data, 13, 4653–4675, https://doi.org/10.5194/essd-13-4653-2021, 2021.

Gillet-Chaulet, F.: Assimilation of surface observations in a transient marine ice sheet model using an ensemble Kalman filter, The Cryosphere, 14, 811–832, https://doi.org/10.5194/tc-14-811-2020, 2020.

GLAMOS: Swiss Glacier Volume Change (release 2023), https://doi.org/10.18750/VOLUMECHANGE.2023.R2023, 2023.

Goldberg, D. N. and Heimbach, P.: Parameter and state estimation with a time-dependent adjoint marine ice sheet model, The Cryosphere, 7, 1659–1678, https://doi.org/10.5194/tc-7-1659-2013, 2013.

Haeberli, W., Alean, J.-C., Müller, P., and Funk, M.: Assessing Risks from Glacier Hazards in High Mountain Regions: Some Experiences in the Swiss Alps, Annals of Glaciology, 13, 96–102, https://doi.org/10.3189/S0260305500007709, 2017.

Hall, D. K., Ormsby, J. P., Bindschadler, R. A., and Siddalingaiah, H.: Characterization of Snow and Ice Reflectance Zones On Glaciers Using Landsat Thematic Mapper Data, Annals of Glaciology, 9, 104–108, https://doi.org/10.3189/S0260305500000471, 1987.

Herrmann, O., Groos, A. R., Tabone, I., Jouvet, G., and Fürst, J. J.: A Kalman filter-based framework for assimilating remote sensing observations into a surface mass balance model, Annals of Glaciology, 66, e23, https://doi.org/10.1017/aog.2025.10020, 2025.

Higdon, D., Pratola, M., Gattiker, J., Lawrence, E., Habib, S., Heitmann, K., Price, S., Jackson, C., and Tobis, M.: Computer Model Calibration using the Ensemble Kalman Filter, http://arxiv.org/abs/1204.3547, arXiv:1204.3547, 2012.

Hock, R., Bliss, A., Marzeion, B., Giesen, R. H., Hirabayashi, Y., Huss, M., Radić, V., and Slangen, A. B. A.: GlacierMIP – A model intercomparison of global-scale glacier mass-balance models and projections, Journal of Glaciology, 65, 453–467, https://doi.org/10.1017/jog.2019.22, 2019.

Hugonnet, R., McNabb, R., Berthier, E., Menounos, B., Nuth, C., Girod, L., Farinotti, D., Huss, M., Dussaillant, I., Brun, F., and Kääb, A.: Accelerated global glacier mass loss in the early twenty-first century, Nature, 592, 726–731, https://doi.org/10.1038/s41586-021-03436-z, 2021.

Huss, M. and Hock, R.: Global-scale hydrological response to future glacier mass loss, Nature Climate Change, 8, 135–140, https://doi.org/10.1038/s41558-017-0049-x, 2018.

Huss, M., Bookhagen, B., Huggel, C., Jacobsen, D., Bradley, R., Clague, J., Vuille, M., Buytaert, W., Cayan, D., Greenwood, G., Mark, B., Milner, A., Weingartner, R., and Winder, M.: Toward mountains without permanent snow and ice, Earth's Future, 5, 418–435, https://doi.org/10.1002/2016EF000514, _eprint: https://agupubs.onlinelibrary.wiley.com/doi/pdf/10.1002/2016EF000514, 2017.

Iglesias, M. A., Law, K. J. H., and Stuart, A. M.: Ensemble Kalman methods for inverse problems, Inverse Problems, 29, 045 001, https://doi.org/10.1088/0266-5611/29/4/045001, 2013.

Islam, N., Carrivick, J. L., Coulthard, T., Westoby, M., Dunning, S., and Gindraux, S.: A growing threat of multi-hazard cascades highlighted by the Birch Glacier collapse and Blatten landslide in the Swiss Alps, Geology Today, 41, 200–205, https://doi.org/10.1111/gto.12526, _eprint: https://onlinelibrary.wiley.com/doi/pdf/10.1111/gto.12526, 2025.

Jouvet, G. and Cordonnier, G.: Ice-flow model emulator based on physics-informed deep learning, Journal of Glaciology, 69, 1941–1955, https://doi.org/10.1017/jog.2023.73, 2023.

Knudsen, L., Park-Kaufmann, H., Corcoran, E., Robel, A., and Mayo, T.: The Potential of the Ensemble Kalman Filter to Improve Glacier Modeling, La Matematica, 3, 1085–1102, https://doi.org/10.1007/s44007-024-00116-y, 2024.

Koboltschnig, G. R. and Schöner, W.: The relevance of glacier melt in the water cycle of the Alps: the example of Austria, Hydrology and Earth System Sciences, 15, 2039–2048, https://doi.org/10.5194/hess-15-2039-2011, 2011.

Maussion, F., Butenko, A., Champollion, N., Dusch, M., Eis, J., Fourteau, K., Gregor, P., Jarosch, A. H., Landmann, J., Oesterle, F., Recinos, B., Rothenpieler, T., Vlug, A., Wild, C. T., and Marzeion, B.: The Open Global Glacier Model (OGGM) v1.1, Geoscientific Model Development, 12, 909–931, https://doi.org/10.5194/gmd-12-909-2019, 2019.

Maussion, F., Rothenpieler, T., Dusch, M., Schmitt, P., Vlug, A., Schuster, L., Champollion, N., Li, F., Marzeion, B., Oberrauch, M., Eis, J., Landmann, J., Jarosch, A., Fischer, A., luzpaz, Hanus, S., Rounce, D., Castellani, M., Bartholomew, S. L., Minallah, S., bowenbe-longstonature, Merrill, C., Otto, D., Loibl, D., Ultee, L., Thompson, S., anton ub, Gregor, P., and zhaohongyu: OGGM/oggm: v1.6.0, https://doi.org/10.5281/zenodo.7718476, 2023.

Millan, R., Mouginot, J., Rabatel, A., and Morlighem, M.: Ice velocity and thickness of the world's glaciers, Nature Geoscience, 15, 124–129, https://doi.org/10.1038/s41561-021-00885-z, 2022.

Otsu, N.: A Threshold Selection Method from Gray-Level Histograms, IEEE Transactions on Systems, Man, and Cybernetics, 9, 62–66, https://doi.org/10.1109/TSMC.1979.4310076, 1979.

RGI Consortium: Randolph Glacier Inventory - A Dataset of Global Glacier Outlines. (NSIDC-0770, Version 7). [Data Set]. Boulder, Colorado USA. National Snow and Ice Data Center., https://doi.org/10.5067/F6JMOVY5NAVZ, 2023.

Rounce, D. R., Hock, R., Maussion, F., Hugonnet, R., Kochtitzky, W., Huss, M., Berthier, E., Brinkerhoff, D., Compagno, L., Copland, L., Farinotti, D., Menounos, B., and McNabb, R. W.: Global glacier change in the 21st century: Every increase in temperature matters, Science, 379, 78–83, https://doi.org/10.1126/science.abo1324, 2023.

Schaefli, B., Manso, P., Fischer, M., Huss, M., and Farinotti, D.: The role of glacier retreat for Swiss hydropower production, Renewable Energy, 132, 615–627, https://doi.org/10.1016/j.renene.2018.07.104, 2019.

Schmitt, P., Maussion, F., Goldberg, D. N., and Gregor, P.: The Open Global Glacier Data Assimilation Framework (AGILE) v0.1, EGUsphere, pp. 1–35, https://doi.org/10.5194/egusphere-2025-3401, 2025.

Slater, T., Lawrence, I. R., Otosaka, I. N., Shepherd, A., Gourmelen, N., Jakob, L., Tepes, P., Gilbert, L., and Nienow, P.: Review article: Earth's ice imbalance, The Cryosphere, 15, 233–246, https://doi.org/10.5194/tc-15-233-2021, 2021.

Sommer, C., Malz, P., Seehaus, T. C., Lippl, S., Zemp, M., and Braun, M. H.: Rapid glacier retreat and downwasting throughout the European Alps in the early 21st century, Nature Communications, 11, 3209, https://doi.org/10.1038/s41467-020-16818-0, 2020.

Sommer, C., Groos, A. R., Fürst, J., and Braun, M.: Transient snow line altitudes of glaciers in the European Alps from multi-mission remote sensing data (2000–2025), Earth System Science Data Discussions, pp. 1–39, https://doi.org/10.5194/essd-2026-35, 2026.

The GlaMBIE Team: Community estimate of global glacier mass changes from 2000 to 2023, Nature, 639, 382–388, https://doi.org/10.1038/s41586-024-08545-z, 2025.

Welty, E., Zemp, M., Navarro, F., Huss, M., Fürst, J. J., Gärtner-Roer, I., Landmann, J., Machguth, H., Naegeli, K., Andreassen, L. M., Farinotti, D., Li, H., and Contributors, G.: Worldwide version-controlled database of glacier thickness observations, Earth System Science Data, 12, 3039–3055, https://doi.org/10.5194/essd-12-3039-2020, 2020.

WGMS: Fluctuations of Glaciers Database. World Glacier Monitoring Service (WGMS), Zurich, Switzerland, https://doi.org/https://doi.org/10.5904/wgms-fog-2024-01, 2024.

Zekollari, H., Schuster, L., Maussion, F., Hock, R., Marzeion, B., Rounce, D. R., Compagno, L., Fujita, K., Huss, M., James, M., Kraaijenbrink, P. D. A., Lipscomb, W. H., Minallah, S., Oberrauch, M., Van Tricht, L., Champollion, N., Edwards, T., Farinotti, D., Immerzeel, W., Leguy, G., and Sakai, A.: Glacier preservation doubled by limiting warming to 1.5°C versus 2.7°C, Science, 388, 979–983, https://doi.org/10.1126/science.adu4675, 2025.